

TWO-DIMENSIONAL QUANTUM MATERIAL IDENTIFICATION VIA SELF-ATTENTION AND SOFT-LABELING IN DEEP LEARNING

Xuan Bac Nguyen¹, Apoorva Bisht¹, Hugh Churchill², Khoa Luu¹

¹ Department of CSCE, University of Arkansas, Fayetteville, AR, USA

² Department of Physics, University of Arkansas, Fayetteville, AR, USA

{xnguyen, abisht, hchurch, khoaluu}@uark.edu

ABSTRACT

In quantum machine field, detecting two-dimensional (2D) materials in Silicon chips is one of the most critical problems. Instance segmentation can be considered as a potential approach to solve this problem. However, similar to other deep learning methods, the instance segmentation requires a large scale training dataset and high quality annotation in order to achieve a considerable performance. In practice, preparing the training dataset is a challenge since annotators have to deal with a large image, e.g 2K resolution, and extremely dense objects in this problem. In this work, we present a novel method to tackle the problem of missing annotation in instance segmentation in 2D quantum material identification. We propose a new mechanism for automatically detecting false negative objects and an attention based loss strategy to reduce the negative impact of these objects contributing to the overall loss function. We experiment on the 2D material detection datasets, and the experiments show our method outperforms previous works.

Index Terms— Quantum images, 2D materials, deep learning, self-attention mechanism, instance segmentation.

1. INTRODUCTION

Two-dimensional (2D) materials hold immense potential for studying optical, electrical, thermal and magnetic properties of materials and exploiting these properties at micro-level. Till now many physical methods [1] like Atomic Force Microscopy [2], High Resolution Transmission Electron Microscopy, Raman Spectroscopy [3], and White Light Contrast Spectroscopy [4] have been used to characterize the dimensions of 2D flakes. However, this is a very tedious process and an experimenter has to manually observe the flakes to determine its characteristics. This requires resources, skills and time. Recently, deep-learning based approaches to identify and characterize 2D flakes have been proposed and few applications have been implemented [5, 6]. The principle for this characterization is that depending on the thickness of the flakes deposited on the dielectric layers, the optical images observed under the microscope show a gradient of

colors. These colors are characteristic of the flake thickness and depend on the material being used. For example, hBN (hexagonal boron nitride) flakes have distinct color profile and similarly graphene has its own distinct color profile. However, there is a bottleneck i.e., an extensive dataset is required to implement a fully functional and accurate deep-learning based application. The dataset consisting of images of flakes needs to be fully annotated. This means that all flakes in an image should be identified, segmented and annotated to train the model without false information.

In addition to identifying the thickness of the flake at specific pixels, the color gradient can be used to determine the quality of flake due to changes in thickness. With more characteristics of 2D flakes identified on the basis of microscope images, a deep-learning model can be trained to characterize not just the thickness, but also the grade and other optical properties of the 2D flakes. This holds great promise to increase efficiency and accuracy of the 2D flake "hunting" process.

To this end, we propose a novel method of instance segmentation that helps to localize the location of 2D quantum materials using optical microscopy. In particular, we focus on solving problem of missing annotation that leads to lower recall and overall performances. Therefore, our contributions in this work can be summarized as follows,

- We introduce a new mechanism based on the attention for automatically detecting the potential objects that do not have annotations. This method can be trained end-to-end together with the full deep learning based detection framework.
- We propose an attention based loss strategy that can assign soft-labels for the objects detected above. This approach helps reduce the gradient impact of these objects contributing to the whole framework, thus increasing the recall and overall performance.

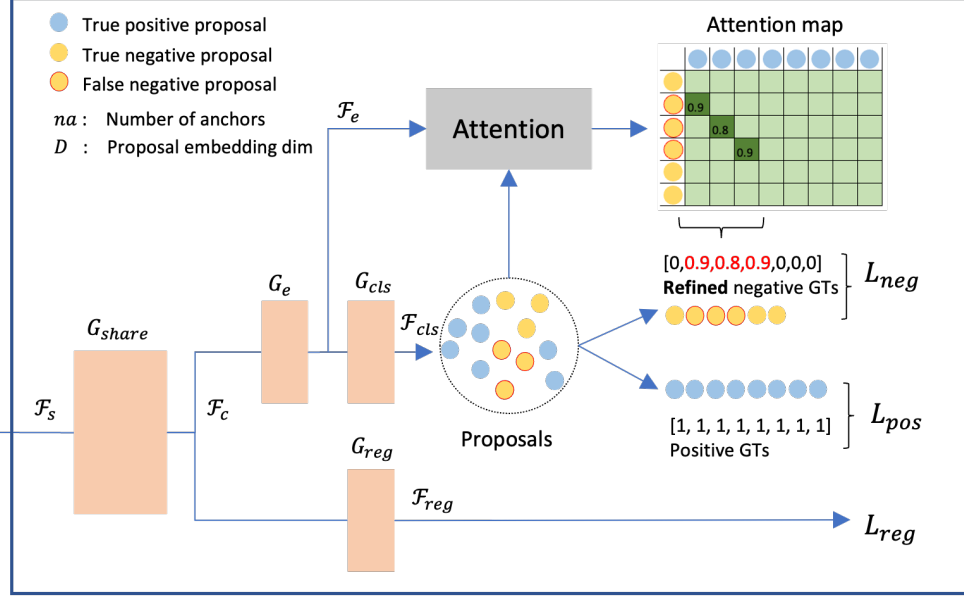


Fig. 1. Our proposed Self-Attention and Soft-Labeling in Region Proposal Network.

2. RELATED WORKS

The previous methods in this topic can be classified into two categories, including traditional and deep learning methods. They will be detailed in the following subsections.

2.1. Prior Works in 2D Quantum Material Identification

A common way to generate 2D flakes is by mechanical exfoliation. These exfoliated flakes are then transferred to substrate like silicon and then observed under the microscope.

AFM (Atomic Force Microscopy): Although AFM can provide resolutions as high as few fractions of nanometer, it requires minute calibrations and has a limited scanning area of 150 by 150 micrometers. [2]. It also has a slow throughput and can damage the crystal lattice during measurement [4].

TEM (Transmission Electron Microscopy): TEM utilizes a high voltage beam of electrons to generate a highly magnified image of the sample. Properties of materials, like the thickness and defects, can be detected and imaged. However, the cost of a typical transmission electron microscope can be as high as \$10 million.

Raman Spectroscopy: Raman spectroscopy uses Raman signals from the materials to determine the thickness. Although a common method to determine thickness of 2D materials, it has its own limitations. Raman spectroscopy gives the thickness of the materials at the location where the light is focused. Thus, in order to determine the thickness at multiple locations, many Raman measurements need to be taken. This is time consuming and is often hard to map the entire flake.

White Light Contrast Spectroscopy: This method increases the contrast between the 2D flake and the substrate by

utilizing the reflection spectrum from normal white light [4].

Among the techniques listed above, some of them have limitations and most of them are expensive and require high maintenance. 2D flake hunting is a basic first step in many research areas. However, currently this first step itself is time consuming and costly.

In subsection 2.2, we describe attempts at using deep learning in 2D quantum materials. These methods are based on a very simple principle, i.e a 2D material has characteristic optical properties at specific thickness. This means for specific substrate - 2D material combination, a color profile can be deciphered which can be used to train a deep-learning model to identify flakes of specific thicknesses.

2.2. Deep Learning in 2D Quantum Materials

The 2D quantum material research topics have gained the attentions from researchers in recent years. In particular, Bingnan et.al [6] proposed a deep learning based optical identification method to recognize 13 different types of 2D materials from optical microscopic images. The method consists of several convolution, batch norm [7], ReLU [8] followed by a softmax layer at the end. The method is inspired by UNet [9] architecture to segment the flakes with different thickness values. Satoru et.al [5] presented an end-to-end pipeline for 2D flakes identification. The method uses optical microscopy images as the input and outputs the locations and material type of each flakes. The authors leverage Mask-RCNN [10] to predict the bounding box, segmentation mask of different types of flake. This method achieves a break-through in field of 2D quantum material detection.

3. OUR PROPOSED METHOD

Our proposed method employs Mask-RCNN [10] as the baseline architecture. It contains three main components namely: Backbone (B), Region Proposal Network (RPN) and Region of Interest Head (ROI). Let $I \in \mathbb{R}^{H \times W \times C}$ be the input image, where H, W, C are height, width and number of channels correspondingly.

The backbone B extracts deep feature maps of I denoted as $\mathcal{F}_s = B(I)$, $\mathcal{F}_s \in \mathbb{R}^{H_s \times W_s \times C_s}$ where s is scale and $H_s = H/s$ and $W_s = W/s$.

Mask-RCNN is a two-stage framework where the results of the first stage will be the input of the second one. It raises a problem that if the first stage is not good enough, the performance of second stage will fall apart. The first stage includes RPN that also nominates the potential objects and their shapes represented by anchors. Apart from prior methods [11] using selective search, RPN can be learnt via back-propagation. In the case of missing annotation, there are objects that do not have any bounding boxes. In a typical way, RPN is confused by treating these potential objects as a background while some similar objects are considered as foreground. In other words, missing annotation is a form of existing *false negative* and leads to *lower recall* of proposing potential objects. As the results, the next second stage will be influenced.

In this paper, our main contribution is to *focus on the RPN to manipulate the missing annotation problem*, enhance the confidence of proposed objects and subsequently improve the next stage as well as overall performance. Our proposed method is illustrated in Fig. 1.

In the first stage, RPN receives \mathcal{F}_s as an input and outputs a list of object proposals \mathcal{P}_s .

$$\mathcal{P}_s = RPN(\mathcal{F}_s) \quad (1)$$

Let na is the number of anchors, total number of proposals that can be generated is $|\mathcal{P}_s| = H_i \times W_i \times na$. \mathcal{P}_s is split into two subsets, i.e. \mathcal{P}_{pos} for positive proposals and \mathcal{P}_{neg} for negative proposals.

$$\mathcal{P}_s = \mathcal{P}_{pos} + \mathcal{P}_{neg}, |\mathcal{P}_s| = H_i \times W_i \times na = |\mathcal{P}_{pos}| + |\mathcal{P}_{neg}| \quad (2)$$

The objectives of RPN are: (1). *Predicting the if a proposal is foreground (1) or background (0)* and (2). *Estimating anchor delta*.

$$\begin{aligned} \mathcal{L}_{RPN} &= \mathcal{L}_{cls} + \mathcal{L}_{reg} \\ &= \frac{1}{|\mathcal{P}_s|} \sum_{p_i \in \mathcal{P}_s} L_{cls}(p_i, \hat{p}_i) + \frac{1}{|\mathcal{P}_{neg}|} \sum_{p_i \in \mathcal{P}_{neg}} L_{reg}(t_i, \hat{t}_i) \end{aligned} \quad (3)$$

where L_{cls} and L_{reg} are the loss functions. p_i is the probability the anchor i^{th} is foreground while \hat{p}_i is the ground truth. Similarly, t_i, \hat{t}_i are predictions and ground truth of anchor size



Fig. 2. The sample of Graphene objects. The red dot circles represents for false negative object without any annotations.

[10] respectively. It is noted that \mathcal{P}_s includes both negative and positive proposals. Thus, in the Eq. (3), \mathcal{L}_{reg} encounters the positive proposals only, while \mathcal{L}_{cls} involves all type of proposals. The \mathcal{L}_{cls} can be reformulated as follows,

$$\begin{aligned} \mathcal{L}_{cls} &= \mathcal{L}_{pos} + \mathcal{L}_{neg} \\ &= \frac{1}{|\mathcal{P}_{pos}|} \sum_{p_i \in \mathcal{P}_{pos}} L_{cls}(p_i, \hat{p}_i) + \frac{1}{|\mathcal{P}_{neg}|} \sum_{p_j \in \mathcal{P}_{neg}} L_{cls}(p_j, \hat{p}_j) \end{aligned}$$

It is clear that $\forall p_i \in \mathcal{P}_{pos}, \hat{p}_i = 1$ and $\forall p_k \in \mathcal{P}_{neg}, \hat{p}_k = 0$. However, dual to missing annotations, it leads to $\exists p_j \in \mathcal{P}_{neg}$ such that $\hat{p}_j = 1$ and p_j is called as *false negative* samples. We propose a mechanism to detect false negative samples automatically. Besides, we present an alternative loss function which uses soft-label for these samples to help reduce gradient impacts to overall architecture. As in Eq. (1), \mathcal{F}_s is the input, RPN is designed as follows,

$$\begin{aligned} \mathcal{F}_c &= G_{share}(\mathcal{F}_s) & \mathcal{F}_{reg} &= G_{reg}(\mathcal{F}_c) \\ \mathcal{F}_e &= G_e(\mathcal{F}_c) & \mathcal{F}_{cls} &= G_{cls}(\mathcal{F}_e) \end{aligned} \quad (4)$$

First, we use a convolution layer G_{share} to create \mathcal{F}_c feature map. It is used to estimate anchor delta values of each anchor by passing to a convolution G_{reg} . Besides, \mathcal{F}_c is also being used to create embedding features \mathcal{F}_e for each anchor using G_e , where G_e denotes the embedding feature.

Given G_{cls} as the probability estimation of every single anchor belongs to foreground or background, it is designed right after G_e in the network. It is noted that $\mathcal{F}_e \in \mathbb{R}^{H_e \times W_e \times (na \times D)}$ and $\mathcal{F}_{cls} \in \mathbb{R}^{H_{cls} \times W_{cls} \times na}$, where D is the dimension of embedding feature and na is the number of anchors. G_{cls} is designed as a convolution with kernel size and stride as 1 to make sure that: $H_e = W_{cls}, H_w = H_{cls}$ and every anchor has its corresponding embedding.

The proposal set \mathcal{P}_s is generated from \mathcal{F}_{cls} and proposals can be identified as either positive or negative ones. We measure the self-attention between two sets of proposal \mathcal{P}_{pos} and \mathcal{P}_{neg} as follows,

$$A = softmax(Norm(\mathcal{F}_{neg}) \odot Norm(\mathcal{F}_{pos})) \quad (5)$$

where $\mathcal{F}_{pos} \in \mathbb{R}^{N_{pos} \times D}$, $\mathcal{F}_{neg} \in \mathbb{R}^{N_{neg} \times D}$ are feature set of all positive and negative proposals. $Norm$ is denoted as the normalization function and \odot is the matrix multiplication. $A \in \mathbb{R}^{N_{neg} \times N_{pos}}$ is the attention map, A_{ij} represents for the similar score between i^{th} negatives and j^{th} positive sample and $\sum_j A_{ij} = 1$. For the false negative proposals, we expect a high A_{ij} score and a low score for the true negative one. We define the threshold t to determine which sample is false negative if $A_{ij} > t$. The loss function for negative proposals is reformulated as follows

$$L_{neg}(p_i, \hat{p}_i) = \begin{cases} L_{cls}(p_i, \max(A_i)), & \text{if } \max(A_i) \geq t \\ L_{cls}(p_i, 0), & \text{if } \max(A_i) < t \end{cases}$$

4. EXPERIMENTS

4.1. Quantum Image Datasets

We use the quantum image dataset published in [5]. The dataset contains 4 type of materials: hBN, Graphene, MoS2, and WTe2. The number of corresponding images for each material are: 353, 862, 569, and 318 images and the number of objects for each material types are: 456, 4805, 839, and 1053 respectively. Fig. 2 shows a sample from dataset.

4.2. Experiment Settings

In our experiments, we use detectron2 framework that is based on Pytorch. We follow the protocol and use the same hyper parameters as described in [12]. More specially, we employ Resnet-101 [13] as the backbone and FPN [14] for multilevel features enhancement. The number of anchors $na = 3$, the feature dimension of anchor's embedding is $D = 256$. We train the network with learning rate as 0.02 in 10000 iterations and gradually decrease 10 times at the milestone of 5000 and 8000 iterations. The batch size is set to 48. The model is trained on a machine of 4GPUs with 48G each. Training time takes 2 hours to finish. We understand that the baseline in [5] uses Keras/Tensorflow implementation, so the model is retrained by using detectron2 as a baseline.

5. RESULTS

The performance of four type of materials is reported in Table 1 following official COCO metrics [15]. Overall, our method outperforms previous methods [5], [12] in terms of average precision of both bounding box and segmentation criteria. More specially, compared to the baseline [5], there are large margins improvements (3% - 5% approximately) in bounding boxes and 3% of increasing in segmentation criteria. Besides, our method outperforms BRL [12] in different type of materials and average precision by 2% approximately.

In addition, we also implement the ablation experiments with different threshold values $t = 0.6, 0.8, 0.9$ to investigate

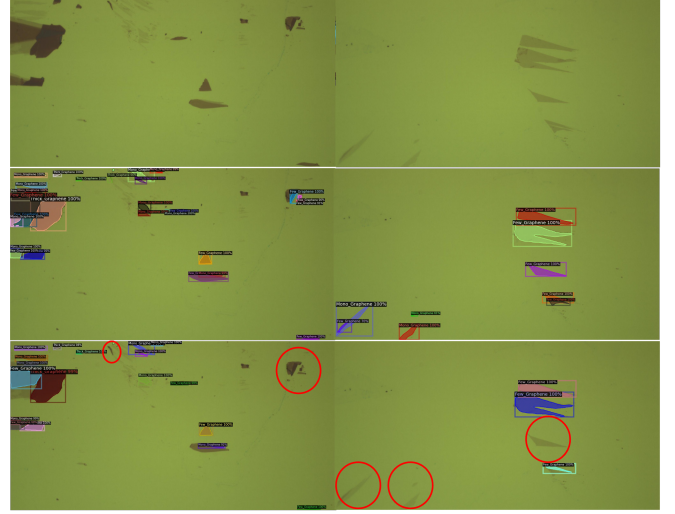


Fig. 3. Qualitative results. The first row is the input images, the second row is our results, and the third row is results of baseline.

how the performance varies. We found that threshold $t = 0.6$ is enough to surpass previous methods and $t = 0.8$ is the optimal values. The qualitative results are shown in Fig. 3.

6. CONCLUSIONS

This work has presented a new approach to tackle the problem of missing annotation in instance segmentation in 2D quantum material identification. A new mechanism has been introduced to detect false negative objects and an attention based loss strategy to reduce their negative impact in the overall loss function. The experimental results on 2D material datasets have shown the advantages of our work compared to prior work by a large margin.

Type	Methods	Bounding Box			Segmentation		
		AP ₅₀	AP ₇₅	AP	AP ₅₀	AP ₇₅	AP
G	Baseline	86.3	78.8	72.4	84.1	71.2	63.2
	OHEM [16]	86.5	79.8	73.1	84.5	71.4	63.7
	BRL [12]	86.8	79.8	73.6	85.1	71.5	63.8
	Ours ($t = 0.6$)	87.1	80.3	74.6	85.0	72.7	64.6
	Ours ($t = 0.8$)	87.8	80.8	75.7	85.7	73.8	65.4
BN	Baseline	73.2	62.0	59.0	73.4	73.2	62.9
	OHEM [16]	71.4	71.0	61.8	71.4	62.0	61.4
	BRL [12]	71.6	71.4	62.8	71.0	69.8	60.8
	Ours ($t = 0.6$)	72.1	72.1	63.7	72.1	71.3	62.7
	Ours ($t = 0.8$)	73.4	73.1	64.4	73.1	72.9	63.0
M	Baseline	60.8	57.0	50.3	60.3	54.3	47.6
	OHEM [16]	62.5	56.1	51.1	61.7	54.1	48.4
	BRL [12]	63.7	59.4	53.7	63.0	57.0	50.6
	Ours ($t = 0.6$)	64.0	57.8	54.2	63.3	57.5	50.9
	Ours ($t = 0.8$)	65.6	60.3	55.1	64.9	58.1	51.9
W	Baseline	76.6	64.8	58.6	74.2	60.7	52.3
	OHEM [16]	76.7	65.3	59.8	75.5	61.2	54.4
	BRL [12]	79.6	66.0	60.6	78.0	61.4	55.0
	Ours ($t = 0.6$)	78.3	65.3	61.4	77.0	64.6	55.9
	Ours ($t = 0.8$)	78.8	67.6	61.8	77.3	63.2	55.3
	Ours ($t = 0.9$)	79.0	68.5	61.2	77.4	65.0	55.4

Table 1. Performance on different types of 2D quantum materials. G: Graphene, BN: hBN, M: MoS₂, W: WeT2

7. REFERENCES

- [1] Ying Ying Wang, Ren Xi Gao, Zhen Hua Ni, Hui He, Shu Peng Guo, Huan Ping Yang, Chun Xiao Cong, and Ting Yu, “Thickness identification of two-dimensional materials by optical imaging,” *Nanotechnology*, vol. 23, no. 49, pp. 495713, nov 2012.
- [2] Suprakas Sinha Ray, “4 - techniques for characterizing the structure and properties of polymer nanocomposites,” in *Environmentally Friendly Polymer Nanocomposites*, Suprakas Sinha Ray, Ed., Woodhead Publishing Series in Composites Science and Engineering, pp. 74–88. Woodhead Publishing, 2013.
- [3] Andrea C Ferrari, Jannik C Meyer, Vittorio Scardaci, Cinzia Casiraghi, Michele Lazzeri, Francesco Mauri, Stefano Piscanec, Dingde Jiang, Konstantin Sergeevich Novoselov, Siegmund Roth, et al., “Raman spectrum of graphene and graphene layers,” *Physical review letters*, vol. 97, no. 18, pp. 187401, 2006.
- [4] Z. H. Ni, H. M. Wang, J. Kasim, H. M. Fan, T. Yu, Y. H. Wu, Y. P. Feng, and Z. X. Shen, “Graphene thickness determination using reflection and contrast spectroscopy,” *Nano Letters*, vol. 7, no. 9, pp. 2758–2763, 2007, PMID: 17655269.
- [5] Satoru Masubuchi, Eisuke Watanabe, Yuta Seo, Shota Okazaki, Takao Sasagawa, Kenji Watanabe, Takashi Taniguchi, and Tomoki Machida, “Deep-learning-based image segmentation integrated with optical microscopy for automatically searching for two-dimensional materials,” *npj 2D Materials and Applications*, vol. 4, no. 1, pp. 1–9, 2020.
- [6] Bingnan Han, Yuxuan Lin, Yafang Yang, Nannan Mao, Wenyue Li, Haozhe Wang, Kenji Yasuda, Xirui Wang, Valla Fatemi, Lin Zhou, et al., “Deep-learning-enabled fast optical identification and characterization of 2d materials,” *Advanced Materials*, vol. 32, no. 29, pp. 2000953, 2020.
- [7] Sergey Ioffe and Christian Szegedy, “Batch normalization: Accelerating deep network training by reducing internal covariate shift,” in *International conference on machine learning*. PMLR, 2015, pp. 448–456.
- [8] Abien Fred Agarap, “Deep learning using rectified linear units (relu),” *arXiv preprint arXiv:1803.08375*, 2018.
- [9] Olaf Ronneberger, Philipp Fischer, and Thomas Brox, “U-net: Convolutional networks for biomedical image segmentation,” in *International Conference on Medical image computing and computer-assisted intervention*. Springer, 2015, pp. 234–241.
- [10] Kaiming He, Georgia Gkioxari, Piotr Dollár, and Ross Girshick, “Mask r-cnn,” in *Proceedings of the IEEE international conference on computer vision*, 2017, pp. 2961–2969.
- [11] Ross Girshick, “Fast r-cnn,” in *Proceedings of the IEEE international conference on computer vision*, 2015, pp. 1440–1448.
- [12] Han Zhang, Fangyi Chen, Zhiqiang Shen, Qiqi Hao, Chenchen Zhu, and Marios Savvides, “Solving missing-annotation object detection with background recalibration loss,” in *ICASSP 2020-2020 IEEE International Conference on Acoustics, Speech and Signal Processing (ICASSP)*. IEEE, 2020, pp. 1888–1892.
- [13] Kaiming He, Xiangyu Zhang, Shaoqing Ren, and Jian Sun, “Deep residual learning for image recognition,” in *Proceedings of the IEEE conference on computer vision and pattern recognition*, 2016, pp. 770–778.
- [14] Tsung-Yi Lin, Piotr Dollár, Ross Girshick, Kaiming He, Bharath Hariharan, and Serge Belongie, “Feature pyramid networks for object detection,” in *Proceedings of the IEEE conference on computer vision and pattern recognition*, 2017, pp. 2117–2125.
- [15] Tsung-Yi Lin, Michael Maire, Serge Belongie, James Hays, Pietro Perona, Deva Ramanan, Piotr Dollár, and C Lawrence Zitnick, “Microsoft coco: Common objects

in context,” in *European conference on computer vision*. Springer, 2014, pp. 740–755.

- [16] Abhinav Shrivastava, Abhinav Gupta, and Ross Girshick, “Training region-based object detectors with on-line hard example mining,” in *Proceedings of the IEEE conference on computer vision and pattern recognition*, 2016, pp. 761–769.